Chemokines in atherosclerotic lesion development and stability : from mice to man

Jager, S.C.A. de

7 Hematopoietic Macrophage Inhibitory Cytokine-1 Deficiency Protects Against Atherosclerosis by Modulating Leukocyte Recruitment and Homeostasis in a Strictly CCR2 and TGFβR-II Dependent Manner

Saskia C.A. de Jager[1]*, Beatriz Bermúdez[2]*, Ilze Bot[1], Vivian de Waard[1], Martine Bot[1], Francisco J.G. Muriana[2], Theo J.C. van Berkel[1], Se-Jin Lee[3], Rocio Abia[2]* and Erik A.L. Biessen[1,4]*

Submitted

Abstract

Objectives: Macrophage inhibitory cytokine-1 (MIC-1) is a distant member of the transforming growth factor β (TGFβ) superfamily, which operates in acute phase responses through a currently unknown receptor. Elevated MIC-1 serum levels were recently shown to be an independent risk factor for acute coronary syndromes. This led us to address the role of this cytokine in atherogenesis.

Methods and results: Irradiated LDLr$^{-/-}$ mice, reconstituted with MIC-1$^{-/-}$ or littermate bone marrow showed impaired lesion formation in the aortic sinus after 4 (initial plaques) but not 12 weeks of western type diet feeding (advanced plaques). Advanced plaques of MIC-1$^{-/-}$ chimeras had reduced macrophage infiltrates, increased collagen deposition and decreased necrotic core formation and intimal apoptosis, all features of improved plaque stability. MIC-1$^{-/-}$ chimeras suffered from mild monocytopenia and a concomitant reduction in stromal monocyte numbers, most notably of the CD11b^{+} Ly6C^{low} CX3CR1^{high} subset, suggestive of perturbed myeloid differentiation. We show that MIC-1$^{-/-}$ macrophages display an impaired CCR2 directed chemotactic response, while conversely MIC-1 induced macrophage chemotaxis appeared to be strictly CCR2 and TGFßRII-dependent.

C**onclusions:** The acute phase protein MIC-1 exerts a multifaceted role in regulating atherosclerosis and plaque stability modulating leukocyte influx and homeostasis. Its activity profile and inflammation driven expression render MIC-1 a very attractive target for plaque stabilizing therapy.

Introduction

The superfamily of Transforming Growth Factor-beta (TGF-β) encompasses two major sub-families: the TGFβ/Activin/Nodal family and the bone morphogenic protein (BMP)/ Growth Differentiation Factor (GDF) subfamily[1]. Transforming growth factor-beta family members are notorious for their pleiotropic effects on cell cycle (proliferation, differentiation and apoptosis), inflammation, cellular motility and adhesion, cartilage/ bone formation and neuronal growth [2, 3]. Generally TGFβ/Activin/Nodal members interact with the common membrane-bound TGFβ receptors 2 (TGFβRII), which consequently dimerizes with TGF-β receptor 1 (TGFβR1), leading to SMAD dependent signaling. After nuclear translocation SMAD complexes interact with co-activators to effect transcriptional activation of several target genes[1], [4, 5]. Members of the BMP/GDF family interact with two serine/threonine kinase receptors (BMPR1 and BMPRII) inducing a signal transduction pathway very similar to that of the TGFβ/Activin/ Nodal family[4, 5]**.** However interaction of BMP with its receptor is not unambiguously established as they have affinity for the classical TGFβ receptors, and most notably for TGFβRI, as well.

Macrophage inhibitory cytokine-1 (MIC-1), also known as Growth Differentiation Factor-15, Placental Bone Morphogenic Protein, Prostate Differentiation Factor and placental TGFβ, is a distant member of the subfamily of Bone Morphogenic Proteins [6, 7]. MIC-1 has alleged anti-inflammatory activity that acts through an unknown receptor. It is weakly expressed under normal conditions[6, 8] but is sharply upregulated under conditions of inflammation[9, 10], where it is shown to act as an autocrine regulator of macrophage activation[6]. Next to its effects on macrophages MIC- 1 was also identified as a downstream target gene of p53, suggesting a role in injury response to DNA damage and cancer. In support of this notion, some studies have indeed shown that MIC-1 is involved in apoptosis of various cancer cells[11, 12], while in other studies MIC-1 was seen to protect cells from apoptosis by inducing cellular S phase arrest[13]. Moreover several anti-cancer drugs are known to induce MIC-1 expression[11, 14, 15].

MIC-1, both tissue-derived and circulating, appeared to be cardio-protective in mouse models for myocardial infarction and heart failure [16, 17]. Conversely, elevated MIC-1 serum levels were shown to be an independent risk factor for acute coronary syndromes[18, 19]. In this study we have therefore addressed the potential involvement of MIC-1 in atherogenesis. We demonstrate that while hematopoietic MIC-1 deficiency attenuated early lesion formation; it also improved atherosclerotic plaque stability by enhancing collagen deposition and decreasing necrotic core expansion.

Materials & Methods

Animals

LDLr$^{-/-}$ mice were obtained from the local animal breeding facility. Mice were maintained on regular chow (RM3; Special Diet Services, Essex, U.K.). Drinking water was provided ad libitum. In vivo experiments were performed at the animal facilities of the Gorlaeus laboratories. All experimental protocols were approved by the ethics committee for animal experiments of Leiden University.

Bone Marrow Transplantation

To induce bone marrow aplasia, male LDLr$^{-/-}$ recipient mice were exposed to a single dose of 9 Gy (0.19 Gy/min, 200 kV, 4 mA) total body irradiation using an Andrex Smart 225 Röntgen source (YXLON International) with a 6-mm aluminum filter 1 day before the transplantation. Bone marrow was isolated from male MIC-1$^{-/-}$ or littermates by flushing the femurs and tibias. Irradiated recipients received 0.5x10^7 bone marrow cells by tail vein injection and were allowed to recover for 6 weeks. Drinking water was supplied with antibiotics (83 mg/L ciprofloxacin and 67 mg/L polymyxin B sulfate) and

6.5 g/L sucrose and was provided ad libitum. Animals were placed on a Western type diet containing 0.25% cholesterol and 15% cacao butter (SDS) diet for 4 and 12 weeks and subsequently sacrificed.

Histological analysis
Cryostat sections of the aortic root (10 μm) were collected and stained with Oil-red-O. Lesion size was determined in 5 sections of the aortic valve leaflet area. Corresponding sections on separate slides were stained immunohistochemically with an antibody directed against a macrophage specific antigen (MoMa-2, monoclonal rat IgG2b, dilution 1:50; Serotec, Oxford, UK). Goat anti-rat IgG-AP (dilution 1:100; Sigma, St. Louis, MO) was used as secondary antibody and NBT-BCIP (Dako, Glostrup, Denmark) as enzyme substrates. Masson's trichrome staining (Sigma) was used to visualize collagen (blue staining). Cellular apoptosis was visualized using a terminal deoxytransferase dUTP nick-end labeling (TUNEL) kit (Roche Diagnostics). Apoptotic nuclei were scored manually. Intimal necrosis was determined by assessment of necrotic area in TUNEL stained sections. Histological analysis was performed by an independent operator.

Flow Cytometry
Bone marrow was isolated by flushing the femurs and tibias with PBS. Subsequently the cell suspension was gently filtered through a 70μm cell strainer to obtain a single cell suspension (BD Falcon, BD Biosciences, San Jose, CA). Peritoneal leukocytes were harvested by peritoneal cavity lavage with PBS. Crude peripheral blood mononuclear cells (PBMC) and peritoneal leukocytes were incubated at 4°C with erythrocyte lysis buffer (155mM NH_4CL in 10mM Tris/HCL, pH 7.2) for 5 minutes. Cells were centrifuged for 5 minutes at 1500 rpm, resuspended in lysis buffer to remove residual erythrocytes. Cells were washed twice with PBS. Cell suspensions were incubated with 1% normal mouse serum in PBS and stained for the surface markers F4/80 antigen, CD11b, CD19, CD4, CD23, CD69, CD86 (eBioscience, San Diego, CA.), CD8, Ly6C (BD Pharmingen, San Diego, CA.), CX3CR1 (MBL, Woburn, MA.) and CCR2 (clone E68, Abcam, Cambridge, MA.) at a concentration of 0.25 μg Ab/200.000 cells. Optionally cells were permeabilized and stained intracellulary for FoxP3, according to the manufacturer's protocol (eBioscience). Subsequently cells were subjected to flow cytometric analysis (FACSCalibur, BD Biosciences, San Diego, CA). FACS data was analyzed with CELLQuest software (BD Biosciences).

Cell Culture
The murine macrophage cell line (RAW 264.7, TIB-71, ATCC) was grown in DMEM (containing 10% Fetal Bovine Serum (FBS), 2 mmol/L L-glutamine, 100 U/ml penicillin, and 100 μg/ml streptomycin) in a humidified atmosphere (5% CO_2) and at 37°C.

Migration Assay
RAW 264.7 were starved for 24 hours in medium containing 1% FBS before the experiment. Serum deprived cells were detached using trypsin-EDTA and $3.5x10^4$ cells were seeded onto transwell inserts (pore size 5 μm; Becton Dickinson Labware). Medium containing the chemotactic stimuli (MIC-1 10ng/ml (R&D system), murine MCP-1 (JE) 10ng/ml (Peprotech, Rocky Hill, NJ), TGFβ1 10ng/ml (Peprotech, Rocky Hill, NJ), with or without TGF-β signaling inhibitors (PI3 kinase inhibitor (Ly294-002, Sigma) 10μM, SMAD-3 inhibitor (SIS3, Sigma) 3μM and ERK inhibitor (PD98059, Sigma) 20μM) was added to the basolateral side of the membrane and cells were allowed to migrate for 24 hours. The chemotactic peptide n-formyl-methionine-leucine-phenylalanine (fMLP, Sigma) was used as a positive control (1 nmol/L). Finally after centrifugation of the plate (5 min, 1000 rpm), RAW 264.7 were fixed and stained with Mayer's Hematoxylin. The number of cells that had completely migrated to the basolateral side of the chamber was scored manually.

Peritoneal leukocytes from WT or $CCR2^{-/-}$ mice were harvested by peritoneal

lavage and contained in complete DMEM to allow cell attachment. Four hours after seeding non adherent cells were removed and adherent cells were gently detached with Accutase (PAA, Gölbe, Germany). Next $1.0x10^5$ peritoneal macrophages were seeded onto 96 well, 8μm pore chemotaxis plates (ChemoTx, Neuroprobe, Gaithersburg, MD) and cells were allowed to migrate for 16 hours in response to MIC-1 and MCP-1 or TGF-β signaling inhibitors. Cells which had completely migrated into the basolateral compartment were counted manually.

Macrophage stimulation
Serum deprived RAW 264.7 macrophages were seeded at a density of approximately 80% and stimulated with recombinant TGFβ-1 (15ng/mL) or MIC-1 (10ng/mL) for 6 hours. Total RNA was isolated for real time PCR. Peritoneal macrophages were harvested by peritoneal lavage and seeded as $0.5 .10^6$ cells/ml. When complete cell adherence was confirmed the cells were stimulated with 100ng/ml LPS (*Salmonella Minnesota* R595 (Re) (List Biological Laboratories Inc., Campbell, CA)) for 24 hours. Subsequently the supernatant was collected and assayed for TGFβ-1 and MCP-1 levels on ELISA, according to the manufacturer's protocol (eBioscience).

Cell Cycle
Cells were serum starved 24 hour before treatments, and then, stimulated with recombinant MIC-1 (10ng/ml), Pifithrin α (Calbiochem, 20nM), p53 inducer (5-Fluorouracil, Sigma aldrich; 25ug/ml) and Recombinant mouse TGFβRII/mouse FC (R&D system, 100ng/mL) for 6, 12 and 24 hours. Cells were harvested, pooled, washed twice in PBS, and fixed in ice-cold 70% ethanol in distilled water for 24 h. Cells were then washed twice in Hank's Balanced Salt Solution (HBSS) and resuspended in PBS containing 0.1 mM EDTA, 0.1% Triton X-100, 50 μg/ml RNAse A and 50 μg/ml PI. After incubation at room temperature for 30 min, cells were analyzed for cell cycle distribution with an EPICS XL flow cytometer (Beckman Coulter) and EXPO32 Software (Beckman Coulter). Red fluorescence (585 nm) was evaluated on a linear scale, and pulse width analysis was used to exclude cell doublets and aggregates from the analysis. Cells with DNA content between 2N and 4N were designated as being in the G1/G0-, S-, or G2/M-phase of the cell cycle. The number of cells in each compartment of the cell cycle was expressed as a percentage of the total number of cells present.

Apoptosis Assay
Cellular apoptosis was measure using a terminal deoxytransferase dUTP nick-end labeling; TUNEL (In situ cell death detection kit, Roche). Cells were serum starved 24 hour before treatments, and then, stimulated with recombinant MIC-1 (10ng/ml) and Pifithrin α (Calbiochem, 20nM) for 24, and 36 hours. Additionally apoptosis was measured by Annexin-V PI staining. Cells were serum starved 24 hour before treatments, and then, stimulated with recombinant MIC-1 (10ng/ml), Pifithrin α (Calbiochem, 20nM), p53 inducer (5-Fluorouracil, Sigma aldrich; 25ug/ml) and Recombinant mouse TGFβRII/mouse Fc (R&D system, 100ng/mL) for 5 days.

Proliferation Assay (MTT)
The cell viability was evaluated with MTT. Briefly, MTT solved in PBS (pH 7.4) was added to the culture media to reach a final concentration of 0,25mg/ml. After the cells were incubated at 37°C for 4h, the culture media containing MTT were removed. Dimethylsulfoxide (DMSO) was added into each well and the absorbance at 540nm was measure by Thermo Labsystems Multiskan Spectrum.

Real time PCR assays
mRNA levels for specific genes were determined by real-time PCR in a MX3000P system (Stratagene). Reverse transcription was performed using three micrograms of RNA and Superscript II RT according to the manufacture's manual. For each PCR, cDNA template was added to Brilliant SYBR green QPCR Master Mix (Stratagene) containing the primer

pairs for CCR2, Cx3CR1, MCP-1, INFγ and PAI-1 (Supplemental table 1). Primers were designed based on PRIMER3.0 (http://frodo.wi.mit.edu/cgibin/primer3/primer3_www.cgiAll) amplification reactions were performed in triplicate and average threshold cycle (Ct) numbers of the triplicates were used to calculate the relative mRNA expression of candidate genes. The magnitude of change of mRNA expression for candidate genes in RAW 267.4 was calculated by using a standard curve. All data were normalized to the gene contents of the endogenous references hypoxanthine phosphoribosyl transferase (HPRT) and glyceraldehyde-3-phosphate dehydrogenase (GAPDH) and expressed as fold change over the controls.

Statistical analysis

Data are expressed as mean ± SEM. A 2-tailed Student's t-test was used to compare individual groups, while multiple groups were compared with a one-way ANOVA and a subsequent Student-Newman-Keuls multiple comparisons test. Non-parametric data were analyzed using a Mann-Whitney U test. A level of $p<0.05$ was considered significant.

Results

Hematopoietic MIC-1 deficiency did not influence body weight or total cholesterol levels throughout the experiment (data not shown). In MIC-1 deficient chimeras MIC-1 expression by peritoneal macrophages and in secondary lymphoid organs such as lymph nodes and spleen was almost completely blunted, while MIC-1 expression in liver was reduced by a significant 60% (Table 1).

	Littermate	**MIC1$^{-/-}$**	***p* value**
Peritoneal Macrophages	1.65 ± 0.54	0.03 ± 0.01	<0.001
Lymph Nodes	0.6 ± 0.53	0.02 ± 0.005	<0.001
Spleen	0.51 ± 0.12	0.07 ± 0.03	<0.001
Liver	2.75 ± 0.50	0.92 ± 0.18	<0.01

Table 1: *Relative MIC-1 expression levels (x10-3) in different cellular components and tissues. Values are expressed as mean ± SEM.*

After recovery mice were put on a Western type diet for 4 and 12 weeks and sacrificed for tissue and aortic leaflet plaque analysis. Early lesion development (4 weeks) was strongly impaired in MIC-1 deficient chimeras (15.8 ± 2.8 in MIC-1$^{-/-}$ vs. 51.5 ± 11.0 x10^3 μm^2 in littermates; p=0.02, Figure 1A), while at week 12 plaque burden was almost equal between littermate and MIC-1$^{-/-}$ bone marrow transplanted mice (232 ± 33 and 174 ± 35 x10^3 μm^2, respectively; p=0.25; Figure 1A/B). However, we did notice striking differences in plaque composition between MIC$^{-/-}$ chimeras and controls at the 12 week time point. Plaque cellularity was significantly decreased in MIC$^{-/-}$ chimeras (1.33 ± 0.11 x10^{-3} vs. 1.94 ± 0.14 cells/μm^2 for controls; p=0.003, Figure 1B). This decrease was at least partially attributable to a decreased plaque macrophage content (30.7 ± 5.6 vs. 45.6 ± 6.1 % for littermate controls; p=0.04, Figure 1C). Next to a decreased inflammatory status plaques of MIC-1 deficient chimeras displayed more pronounced collagen deposition (18.2 ± 1.5 in MIC$^{-/-}$ vs. 11.4 ± 2.5 % in littermates; p=0.04, Figure 2A). Furthermore necrotic core area was significantly smaller in MIC-1$^{-/-}$ bone marrow transplanted mice (13.3 ± 4.2 vs. 29.1 ± 4.2 % in littermates; p=0.02, Figure 2B) as was the rate of intimal apoptosis (1.1 ± 0.35 vs. 2.3 ± 0.35 % in littermates, p=0.03, Figure 2C).

One of the most remarkable features of MIC-1 deficiency was the dramatic reduction of necrotic core size, which was paralleled by a reduced apoptotic rate. As MIC-1 has been implicated in apoptosis, mainly secondary to p53 induction[13], we assessed whether MIC-1 was able to influence macrophage cell homeostasis. Exposure of RAW

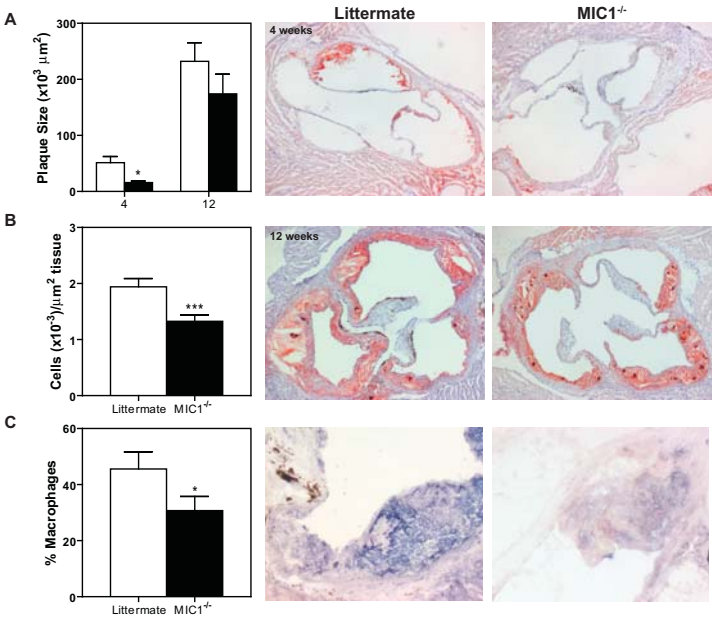

Figure 1: *Effects of MIC-1 Deficiency on Atherogenesis and Plaque Cellularity. Initial plaque development (week 4) was sharply attenuated in MIC-1 deficient chimeras (A), while in progressed plaques (week 12), plaque burden did not differ between littermate and MIC1$^{-/-}$ recipients (representative pictures 50x magnigication panel A, B). Plaque cellularity was significantly decreased in MIC1$^{-/-}$ chimeras (B), which was at least partly due to a decrease in plaque macrophages (C, representative pictures 200x magnification). *p<0.05, ***p<0.001, compared to littermate control.*

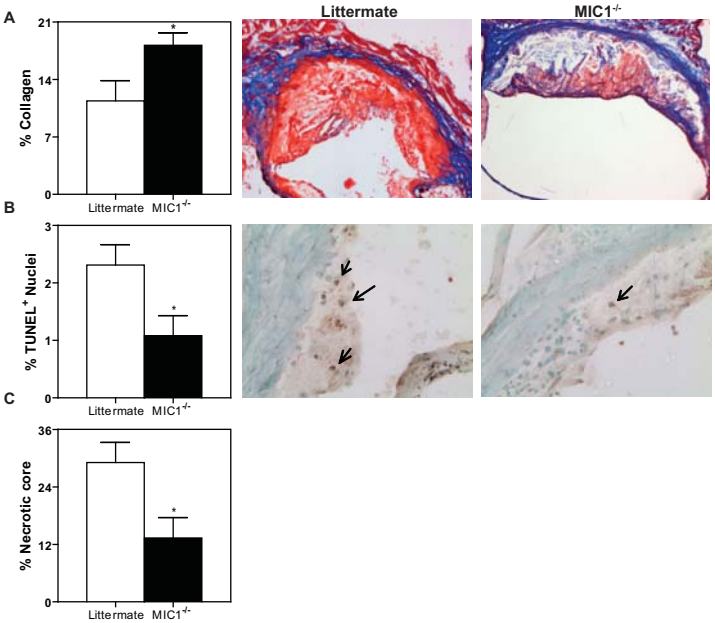

Figure 2: *Effects of MIC-1 Deficiency on Plaque Stability. Advanced plaques (week 12) of MIC-1 deficient chimeras displayed a more stable phenotype with increased collagen content (A, including representative pictures, 100x magnification), decreased necrotic core (C) and attenuated cellular apoptosis (B, including representative pictures, 200x magnification). *p<0.05, compared to littermate control.*

264.7 macrophages to recombinant MIC-1 stimulated S to G2 transition, as analysed by flow cytometry (13.1 ± 0.25 in controls vs. 20.7 ± 0.15 % in MIC-1 treated cells, $p<0.001$ and 6.6 ± 0.12 in controls vs. 21.2 ± 0.21 % in MIC-1 treated , $p<0.001$ after 12 and 24 hours respectively). This effect was completely TGFβRII dependent (20.7 ± 0.15 in MIC-1 compared to 9.2 ± 0.12 % in α-TGFβRII treated cells, $p<0.001$ and 21.2 ± 0.21 in MIC-1 and 3.7 ± 0.09 % in α-TGFβRII treated cells, $p<0.001$ after 12 and 24 hours respectively; Figure 3A). Cell cycle transition was not accompanied by an enhanced proliferative capacity of MIC-1 stimulated macrophages (Figure 3C). Furthermore MIC-1 did not augment p53 induced apoptosis in macrophages (Figure 3D). MIC-1 stimulation for 36h or 5 days did not affect macrophage apoptosis, as assessed by TUNEL staining (Figure 3E). TGFβRII blockade had a moderately stimulatory effect on macrophage apoptosis (5.97 ± 0.09 % in controls vs. 10.67 ± 0.23 % in α-TGFβRII treated macrophages, $p<0.001$; Figure 3F). Moreover MIC-1 was unable to augment p53 induced apoptosis, but interestingly slightly attenuated the induced apoptosis (49.17 ± 0.64 in p53 treated macrophages compared to 42.97 ± 1.16 % in p53/MIC-1 co-stimulated cells, $p<0.001$; Figure 3G). These findings plead for a prominent role of MIC-1 in cell cycle homeostasis rather than in apoptosis as has been proposed recently[20].

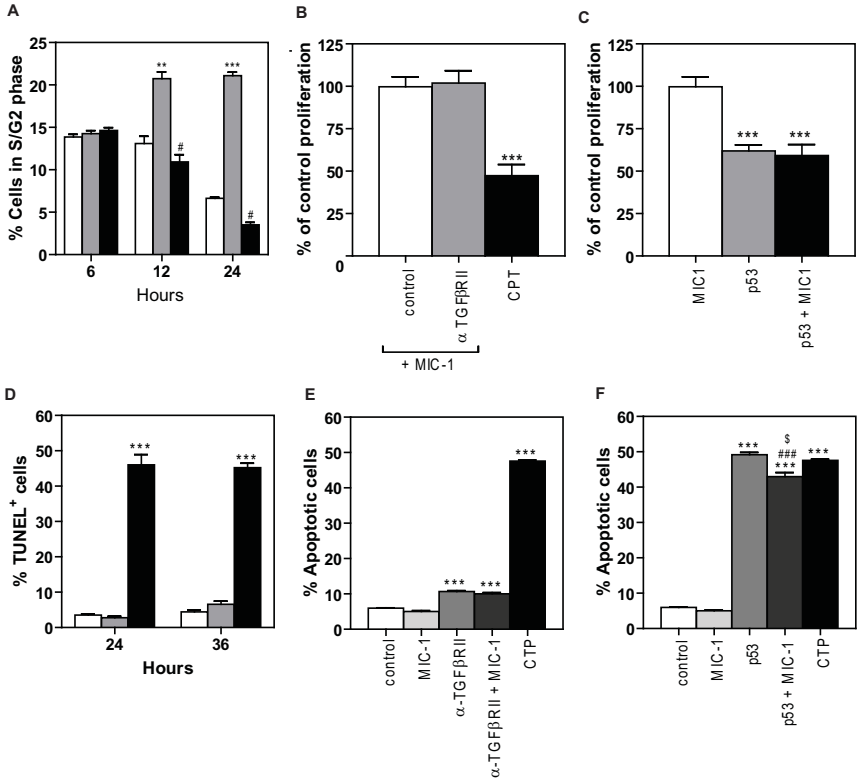

Figure 3: *Cell cycle and apoptosis in MIC-1 treated macrophages. (A) Cell cycle analysis in RAW 264.7 macrophages in control (white) and MIC-1 treated cells (grey) in combination with TGFβRII blockade (black) (B) Cellular proliferation as a percentage of control proliferation in response to MIC-1 (white) in combination with TGFβRII blockade (bar). CTP is used as a positive control (black). (C) Inhibition of cell proliferation by the p53 inducer 5-Fluorouracil (grey) in combination with MIC-1 (black) (D) Apoptosis induction in RAW 264.7 in control (white) MIC-1 treated cells (grey) and CTP treated cells (black), represented as TUNEL positive apoptotic cells. (E) Apoptosis induction after long term (5 day) exposure to control (white), MIC-1 (light grey), α-TGFβRII (intermediate grey), MIC-1 + α-TGFβRII (dark grey) and CTP (black). (F) Apoptosis induction after long term (5 day) exposure to control (white), MIC-1 (light grey), inducer of p53 mediated apoptosis: 5-Fluorouracil (intermediate grey), MIC-1 + p53 (dark grey) and CTP (black). **p<0.01, ***p<0.001 compared to control, #p<0.001 compared to MIC-1, ###p<0.001 compared to p53, $p<0.01 compared to CTP.*

A second striking phenomenon was the reduced presence of macrophages in plaques of MIC-1$^{-/-}$ chimeras. Interestingly, circulating monocyte and peritoneal macrophage counts were also considerably reduced in MIC-1$^{-/-}$ chimeras (2.4 ± 0.3 % vs. 3.8 ± 0.5 in littermate controls; p=0.03, Figure 4A and 0.29 ± 0.04 vs. 0.56 ± 0.10 x10^6 cells/ml in littermate controls, p=0.02, Figure 4B), while no effects were noticed on circulating T cell numbers (data not shown). Hematopoietic MIC-1$^{-/-}$ deficiency did not alter macrophage phenotype (Table 2) as shown by FACS analysis for macrophage phenotype and activation markers including CD86 (classical activation, M1) and CD23 and CD163 (alternative activation, M2[21, 22]).

	Littermate	MIC-1$^{-/-}$	*p* value
M2 Macrophages			
CD23	52.7 ± 3.5 %	52.8 ± 5.1 %	0.98
CD163	51.3 ± 3.3 %	55.9 ± 4.4 %	0.42
M1 Macrophages			
CD86	23.2 ± 5.5 %	22.2 ± 4.0 %	0.88

Table 2: *Peritoneal M1/M2 Macrophage balance in littermate and MIC-1$^{-/-}$ mice. Values are expressed as Mean ± SEM.*

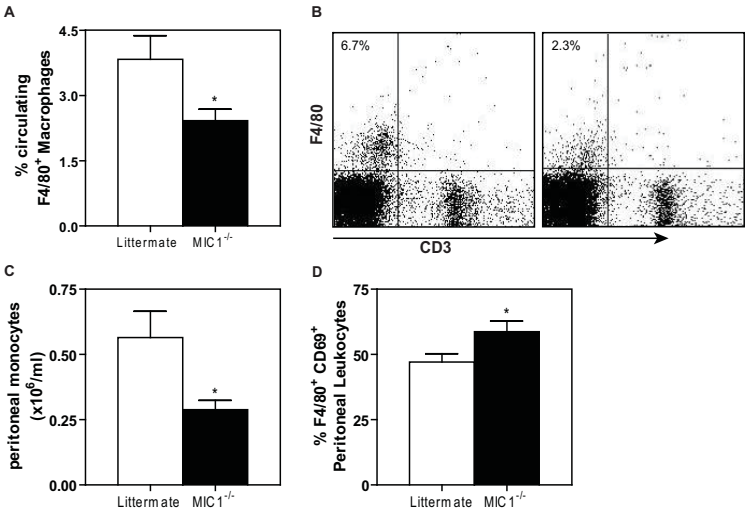

Figure 4: *Monocytopenia in MIC1$^{-/-}$ chimeras. The number of circulating macrophages (A and B; representative FACS plots) and peritoneal monocytes (C) was significantly decreased in the MIC-1 deficient chimeras. Peritoneal monocytes were isolated by peritoneal lavage and differentiated by morphology on Sysmex cell differentiation apparatus. Macrophage activation however was moderately enhanced in MIC-1 deficient chimeras (D). *p<0.05.*

However, FACS analysis for the early macrophage activation marker CD69 did reveal a significant increase of CD69$^+$ cells in the peritoneum, reflective of an enhanced macrophage activation in MIC-1 deficient chimeras (58.7 ± 4.05 % vs. 47.1 ± 3.16 in littermate controls; p=0.04, Figure 4C). To further on this we quantified the expression of pro- and anti-inflammatory mediators in macrophages from controls and MIC-1$^{-/-}$ chimeras. Peripheral blood mononuclear cells and peritoneal leukocytes were analyzed for mRNA expression of a range of -inflammatory and/or chemotactic mediators. Interestingly MIC-1$^{-/-}$ leukocytes displayed an increased MCP-1 expression (Figure 5C/F), while that of its cognate receptor CCR2 was downregulated (Figure 4A/D). The fractalkine receptor CX_3CR1 was significantly downregulated in MIC-1 deficient leukocytes as well (Figure 5 B/E) as was the expression of pro-inflammatory cytokine IFNγ (Figure 5C/E), whereas that of TGFβ was enhanced (Supplemental Figure 1). In

agreement with the latter, ex vivo stimulation of peritoneal macrophages with the TLR-4 ligand lipopolysaccharide (LPS) gave a more pronounced induction of TGF-β release by MIC-1 deficient than by WT macrophages (Supplemental Figure 1, page 126).

As recently shown by Tsou *et al*. CCR2 is instrumental in monocyte egress from bone marrow[23]. Conceivably, the reduction of circulating monocyte numbers as well as that of CCR2 expression by circulating leukocytes may both reflect a perturbed stromal monocyte release. Flow cytometric analysis of bone marrow cells however revealed a similar 40% decrease of stromal $CCR2^+$ cell content in MIC-$1^{-/-}$ chimeras (5.4 ± 0.7 % vs. 9.2 ± 1.8 in littermates ; p=0.04, Figure 6A), establishing that CCR2+ monocytes are not selectively retained in bone marrow of MIC-$1^{-/-}$ chimeric mice. Indeed, total $CX3CR1^+$ monocyte numbers in bone marrow tended to be reduced as well (-25%, Figure 6B).

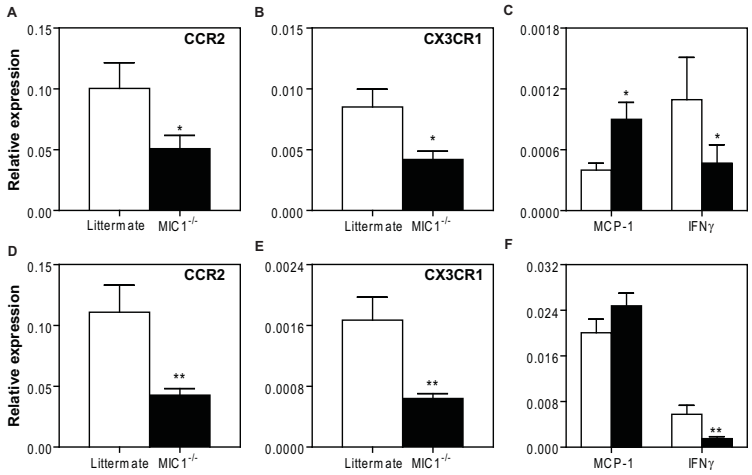

Figure 5: *Pro and anti-inflammatory mediators in MIC1$^{-/-}$ macrophages. Relative mRNA expression of CCR2 (A, C) and CX3CR1 (B, D), MCP-1 and IFNγ (C, E; littermate (white bars) and MIC-1$^{-/-}$ mice (black bars) in PBMC (A,B,C) and peritoneal macrophages (D,E,F). Values are expressed relative to GAPDH and HPRT expression. *p<0.05, **p<0.01.*

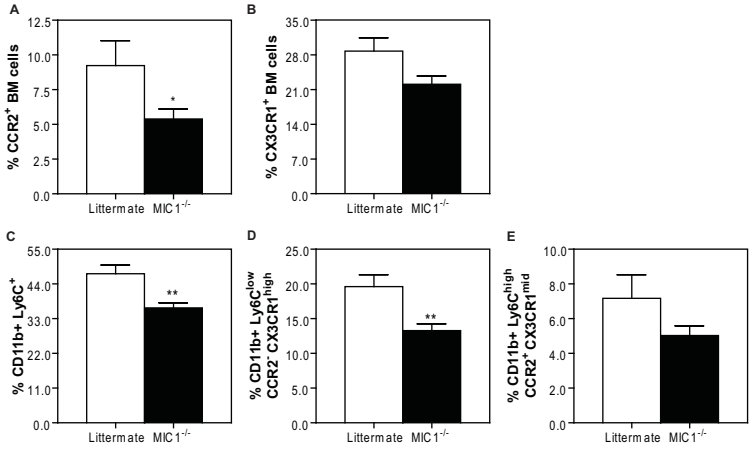

Figure 6: *Effects of MIC-1 on stromal monocyte subsets. The bone marrow of MIC $^{-/-}$ chimeras contained less CCR2 and CX3CR1 expressing cells. Moreover the percentage of $CD11b^+$ $Ly6C^+$ monocytes is decreased in bone marrow of MIC-1$^{-/-}$ recipients (C). Further analysis revealed that the $Ly6C^{low}$ $CCR2^-$ $CX3CR1^{high}$ cell population was particularly affected (D) while the $Ly6C^{high}$ $CCR2^+$ $CX3CR1^{mid}$ population remained largely unaltered (E). *p<0.05, **p<0.01*

Recently two Ly6C^{+} monocyte subsets have been identified with divergent chemotactic and phagocytotic properties[24]. The Ly6C^{high} CCR2^{+} CX3CR1^{mid} population preferentially accumulates in atherosclerotic plaques, while Ly6C^{low} CCR2^{-} CX3CR1^{hi} cell migration into plaques is a less frequent event. The latter population readily differentiates into CD11c expressing phagocytes. In our study MIC-1 deficiency appeared to affect the total Ly6C monocyte population in bone marrow (36.4 ± 1.6 % vs. 47.2 ± 2.7 in littermates; p=0.004, Figure 6C), albeit that this reduction was more pronounced for Ly6C^{low} CCR2^{-} CX3CR1^{high} than for Ly6C^{+}CCR2^{+}CX3CR1^{mid} cells (13.3 ± 1.0 % vs. 19.6 ± 1.7 in littermates; p=0.006, Figure 6D). We did not observe any differences between the two subsets in the circulation nor in the peritoneal cavity. Collectively our data indicate that MIC-1 deficiency unlikely affects atherogenesis by lowering the release of a particular monocyte subset from the bone marrow or by perturbing the balance between Ly6C^{low} phagocytes and Ly6C^{high} pro-inflammatory monocytes.

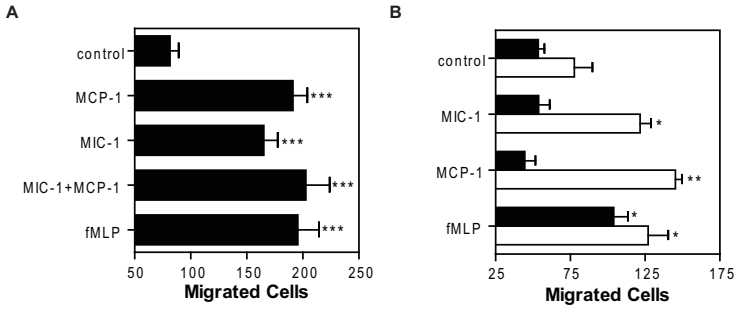

Figure 7: *Macrophage Migration response towards MIC-1. (A) Ex Vivo migration of WT peritoneal macrophages in response to MCP-1, MIC-1 or a combination of both. (B) Ex Vivo migration of C57Bl6 (white bars) and CCR2 (black bars) deficient peritoneal macrophages towards recombinant MIC-1 and MCP-1. *p<0.05, **p<0.01, ***p<0.001, compared to control.*

Altogether the intriguing notion emerges that the reduced accumulation of MIC-1$^{-/-}$ monocytes in the plaque may be related to the observed effects on CCR2 chemokine receptor function. This is also compatible with our finding that like CCR2, MIC-1 deficiency has a more profound impact on plaque initiation than on progression[25]. To validate this hypothesis we performed chemotaxis assays in order to elucidate effects of MIC-1 deficiency on monocyte migration. To our surprise MIC-1 appeared to be equally effective in promoting peritoneal macrophage cell migration as MCP-1 (Figure 7A). Co-stimulation of peritoneal macrophages with MIC-1 and MCP-1 did not lead to an augmented response, pointing to convergent pathways (Figure 7A). To verify whether MIC-1 interferes with CCR2 signaling at a different level, chemotaxis assays were conducted for CCR2 deficient macrophages. Migration towards MCP-1 was, as expected, largely blunted in CCR2 deficient cells. Surprisingly MIC-1 was unable to induce CCR2$^{-/-}$ cell migration as well, whereas the migratory capacity of the chemotactic peptide fMLP was unaltered in CCR2$^{-/-}$ cells (Figure 7B). These findings point to a direct interaction of MIC-1 with chemokine receptor CCR2 function. In a next step we measured LPS induced release of MCP-1 by MIC-1 deficient vs. WT macrophages to evaluate whether CCR2 function was impaired as result of a negative feedback response to elevated MCP-1 levels. While LPS treatment induced massive MCP-1 release in both WT and MIC-1 deficient macrophages, MCP-1 release by MIC-1 deficient cells was essentially similar to that of WT cells, suggesting that CCR2 responsiveness rather than pericellular MCP-1 release underlies the observed CCR2 dependent mobility in MIC-1$^{-/-}$ macrophages (Supplemental Figure 1).

Recombinant MIC-1 and TGFβ-1 both induced the expression of an established TGFβ responsive gene Plasminogen Activator Inhibitor-1 in RAW 264.7 macrophages (Figure 8A), indicating that MIC-1 displays a similar capacity to activate TGFβ receptor II

as TGFβ itself. The latter however only moderately increased induced MCP-1 expression, while MIC-1 did so robustly (Figure 8A). Moreover MIC-1 induced MCP-1 expression was prevented by co-incubation with a SMAD-3 inhibitor (Figure 8B). Furthermore while TGFβ receptor I blockade did not influence MCP-1 expression, blockade of TGFβ receptor II completely abrogated the MIC-1 induced MCP-1 production (Figure 8C). This indicates that MIC-1 induces MCP-1 expression by activating TGFβ signaling, via the common TGFβ receptor II in a TGFβ receptor I independent manner. *In vitro* migration with RAW 264.7 macrophages confirmed that MIC-1, at least partially, signals via the TGFβ pathway as its response was completely abrogated by PI3 kinase, SMAD-3 and ERK inhibitors (Figure 8D). *Ex vivo* migration of WT macrophages towards MIC-1 and MCP-1 revealed that MIC-1 dependent migration was not influenced by PI3 kinase inhibition, whereas SMAD-3 appeared the major downstream signaling partner for MIC-1(Figure 8E). Furthermore MCP-1 induced migration showed similar regulation by SMAD-3 as MIC-1.

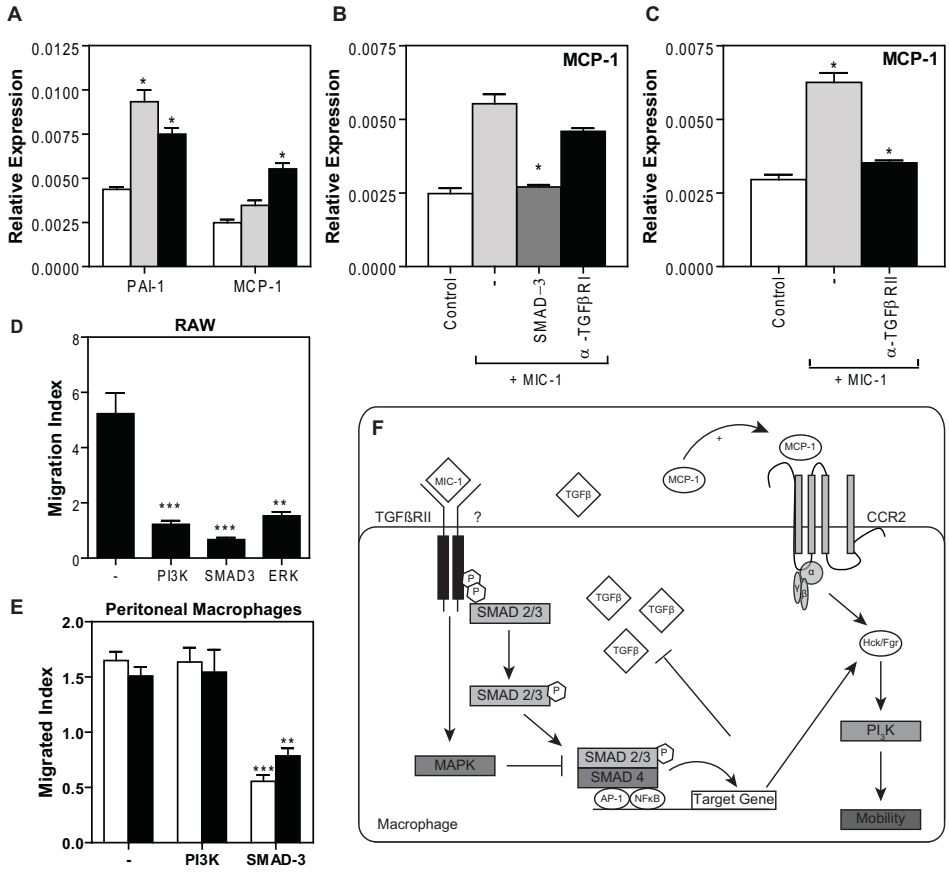

Figure 8: *Similar signaling pathways of MIC-1 and TGFβ. (A) Relative expression(to GAPDH and HPRT) of the TGFβ inducible gene PAI-1 and MCP-1 in control (white bars), TGFβ (grey bars) and MIC-1 (black bars) stimulated macrophages. MCP-1 expression by MIC-1 can be inhibited by a SMAD-3 inhibitor (dark grey bar, B) and TGFβRII blockade (light grey and white bar, C). (D) MIC-1 induced migration in RAW macrophages can be inhibited with a PI3 kinase (Ly294-002), SMAD3 (SIS3) and ERK (PD98059) inhibitor. Values are corrected for control (medium alone) migration. (E) Ex vivo migration of WT macrophages towards MIC-1 (whit bars) or MCP-1 (black bars) was sharply reduced by SMAD3 inhibition (SIS3), whereas PI3K inhibition (Ly294-002) was not effective. Values are corrected for control (medium alone) migration. (F) Proposed signaling pathway of MIC-1 in macrophages. *p<0.05, ***p<0.001.*

Collectively our data indicate that MIC-1 and TGFβ signaling in macrophages are interrelated. It is conceivable that MIC-1 and TGFβ share mutual intracellular signaling participants. Our data also point to a negative feedback response of MIC-1 on TGFβ, as the absence of MIC-1 resulted in enhanced TGFβ production and release by macrophages. Overall we can conclude that MIC-1 bind and signals via TGFβRII, thereby influencing not only cell cycle processes but also enhancing cellular mobility by regulating downstream signaling of CCR, likely by induction of Src Kinases like Hck or possibly by preventing its desensitization via G Protein Coupled Receptor Kinases (Figure 8F).

Discussion

Macrophage Inhibitory Cytokine-1 is a distant member of the TGFβ superfamily [6, 8], which is notorious for its pleiotropic mode of action. Also its contribution to cardiovascular disorders such as atherosclerosis is complex and poorly understood. MIC-1 was recently shown to be cardio-protective in mouse models for myocardial infarction and heart failure [16, 17], and circulating MIC-1 protected the heart from ischemic injury [17]. Conversely, allelic MIC-1 mutations have been shown to associate with inflammatory disorders such as severe, treatment resistant chronic rheumatoid arthritis[26], while elevated MIC-1 serum levels are an independent risk factor for acute coronary syndromes[18, 19].

In this study we are the first to show that a deficiency of MIC-1 in hematopoietic cells attenuates lesion initiation and improves atherosclerotic plaque stability in more advanced stages of disease development. We show that this is at least partly attributable to a modulation of the inflammatory status and to CCR2 dependent monocyte influx into the plaque. The beneficial effect of MIC-1 deficiency contrasts with that of other TGFβ family members such as activin-A[27] and TGFβ-1, where neutralization resulted in accelerated atherosclerosis and plaque destabilization with reduced collagen deposition and a more pro-inflammatory phenotype[28, 29]. Furthermore specific disruption of TGFβRII signaling aggravated atherogenesis and, again, shifted lesion composition towards a more unstable phenotype[29, 30]. Our studies show that despite the partially contrasting effects of TGFβ and MIC-1, the latter appeared to be a specific trigger of CCR2 signaling, the effects of which can be largely prevented by blocking TGFβRII but not TGFβRI. In fact MIC-1 deficiency was even seen to increase LPS induced TGFβ-1 production by macrophages without noticeably altering macrophage polarization. This could at least partly explain the plaque stabiling effects of hematopoietic MIC-1 deficiency.

Recently Schlittenhardt *et al*. showed that MIC-1 co-localizes with oxidized LDL in the atherosclerotic plaque and contributes to the local oxidative stress and ensuing apoptosis[31]. In keeping with these findings we now demonstrate that plaques from MIC-1$^{-/-}$ chimeras contain less inflammatory cells and in particular less macrophages. The amount of collagen however was significantly increased, which concurs with the significantly lower rate of macrophage apoptosis in the plaque. Reduced macrophage apoptosis may also underlie the smaller necrotic core size in MIC-1$^{-/-}$ chimeras. In this regard our data are in line with the notion that MIC-1 is an acute phase protein that acts in response to p53 dependent injury[13]. Furthermore p53 dependent apoptosis was recently identified as major modulator of atherosclerotic plaque stability, in that p53 deletion enhanced atherogenesis[32, 33], while overexpression in cap cells of advanced atherosclerotic lesions induced plaque rupture[32]. Thus, our findings clearly recapitulate the relevance of the p53/MIC-1 axis for plaque stability. Although pro-apoptotic activity of MIC-1 has been demonstrated in many studies, we were unable to establish any effects of MIC-1 on macrophage apoptosis. Nevertheless, we did observe a direct link between MIC-1 and S > G2 phase transition in macrophages, which was completely TGFβRII dependent. From these data we can conclude that, at least in macrophages, MIC-1 is mainly involved in cell cycle regulation rather than apoptosis. Plausibly, lack of MIC-1 will then lead to cell cycle arrest and subsequent loss of cellular mobility. Collectively, MIC-1 appears to exert its pro-atherogenic effects mainly by TGFß signaling, suggesting

that MIC-1 may in fact act as an acute phase modifier of TGFß activity.

In MIC-$1^{-/-}$ chimeras we did observe a decreased presence of macrophages within the peritoneum and of monocytes in the circulation. Furthermore we show that MIC-$1^{-/-}$ macrophages express lower levels of CCR2 and CX3CR1, while the expression of MCP-1 is increased, possibly due to a compensatory feedback effect. MIC-$1^{-/-}$ macrophages were seen to display both an impaired motility and a chemotactic response to MCP-1. Further study revealed that MIC-1 deficiency is accompanied by reduced CCR2 function, but does not favor macrophage polarization toward either M1 or M2. Most likely the decreased CCR2 sensitivity involves SMAD-3 signaling via the common TGFβ receptor type II. Plaques in MIC-$1^{-/-}$ chimeric mice were typified by increased collagen content. As stimulation of MIC deficient macrophages with LPS led to more pronounced TGFβ production and as TGFβ favorably affects plaque stability[28-30] by inducing vascular smooth cell proliferation[20] and collagen deposition[27,28], it is tempting to assume that MIC-1 deficiency promotes collagen accumulation in a TGFß dependent manner.

In conclusion, we are the first to demonstrate that leukocyte deficiency of MIC-1 improves atherosclerotic plaque stability by impairing macrophage migration, inducing collagen deposition as a result of enhanced TGFβ-1 levels, and decreasing intimal apoptosis. In agreement we show that MIC-$1^{-/-}$ macrophages display a reduced migratory capacity, at least partly by impairing CCR2 function in a TGFß receptor dependent manner. Finally we identify a direct interaction of MIC-1 with TGFβRII signaling. Given also the rather exclusive expression of MIC-1 during acute phase responses and inflammatory conditions, our data suggest that focal inhibition of MIC-1 could be a particularly attractive approach to improve plaque stability by simultaneously quenching CCR2 activity, intimal apoptosis and inducing collagen deposition, which is not associated by the deleterious side effects observed with TGFβ therapy. Furthermore MIC-1 could be an appealing target for the treatment of restenosis as inhibition of MIC-1 influences inflammatory cell recruitment and prevents apoptosis, which are regarded as major culprits for this pathology.

Acknowledgements
The authors like to thank Josan Krom and Lidija Seslija from the division of Biopharmaceutics of the Leiden Amsterdam Center for Drug Research for technical assistance. This work was supported by the Netherlands Heart Foundation (grant D2003T201, S.C.dJ, E.A.B.), Marie Curie Grant (PIEF-GA-2008-221836, B.B.) and to the Spanish Ministry of Science and Education Grant (AGL2005-03722, RA). EAB is an Established Investigator of the Netherlands Heart Foundation (D2003T201).

References

1. Shi Y, Massague J. Mechanisms of TGF-beta signaling from cell membrane to the nucleus. *Cell.* 2003;113(6):685-700.
2. Massague J. TGF-beta signal transduction. *Annu Rev Biochem.* 1998;67:753-791.
3. Massague J, Blain SW, Lo RS. TGFbeta signaling in growth control, cancer, and heritable disorders. *Cell.* 2000;103(2):295-309.
4. Hogan BL. Bone morphogenetic proteins in development. *Curr Opin Genet Dev.* 1996;6(4):432-438.
5. Liu A, Niswander LA. Bone morphogenetic protein signalling and vertebrate nervous system development. *Nat Rev Neurosci.* 2005;6(12):945-954.
6. Bootcov MR, Bauskin AR, Valenzuela SM, Moore AG, Bansal M, He XY, Zhang HP, Donnellan M, Mahler S, Pryor K, Walsh BJ, Nicholson RC, Fairlie WD, Por SB, Robbins JM, Breit SN. MIC-1, a novel macrophage inhibitory cytokine, is a divergent member of the TGF-beta superfamily. *Proc Natl Acad Sci U S A.* 1997;94(21):11514-11519.
7. Bottner M, Laaff M, Schechinger B, Rappold G, Unsicker K, Suter-Crazzolara C. Characterization of the rat, mouse, and human genes of growth/differentiation factor-15/macrophage inhibiting cytokine-1 (GDF-15/MIC-1). *Gene.* 1999;237(1):105-111.
8. Bottner M, Suter-Crazzolara C, Schober A, Unsicker K. Expression of a novel member of the TGF-beta superfamily, growth/differentiation factor-15/macrophage-inhibiting cytokine-1 (GDF-15/MIC-1) in adult rat tissues. *Cell Tissue Res.* 1999;297(1):103-110.
9. Hsiao EC, Koniaris LG, Zimmers-Koniaris T, Sebald SM, Huynh TV, Lee SJ. Characterization of growth-differentiation factor 15, a transforming growth factor beta superfamily member induced following liver injury. *Mol Cell Biol.* 2000;20(10):3742-3751.
10. Schober A, Bottner M, Strelau J, Kinscherf R, Bonaterra GA, Barth M, Schilling L, Fairlie WD, Breit SN, Unsicker K. Expression of growth differentiation factor-15/ macrophage inhibitory cytokine-1 (GDF-15/MIC-1) in the perinatal, adult, and injured rat brain. *J Comp Neurol.* 2001;439(1):32-45.
11. Lim JH, Park JW, Min DS, Chang JS, Lee YH, Park YB, Choi KS, Kwon TK. NAG-1 up-regulation mediated by EGR-1 and p53 is critical for quercetin-induced apoptosis in HCT116 colon carcinoma cells. *Apoptosis.* 2007;12(2):411-421.
12. Rohde M, Daugaard M, Jensen MH, Helin K, Nylandsted J, Jaattela M. Members of the heat-shock protein 70 family promote cancer cell growth by distinct mechanisms. *Genes Dev.* 2005;19(5):570-582.
13. Agarwal MK, Hastak K, Jackson MW, Breit SN, Stark GR, Agarwal ML. Macrophage inhibitory cytokine 1 mediates a p53-dependent protective arrest in S phase in response to starvation for DNA precursors. *Proc Natl Acad Sci U S A.* 2006;103(44):16278-16283.
14. Huang MT, Chen ZX, Wei B, Zhang B, Wang CH, Huang MH, Liu R, Tang CW. Preoperative growth inhibition of human gastric adenocarcinoma treated with a combination of celecoxib and octreotide. *Acta Pharmacol Sin.* 2007;28(11):1842-1850.
15. McDermott DH, Fong AM, Yang Q, Sechler JM, Cupples LA, Merrell MN, Wilson PW, D'Agostino RB, O'Donnell CJ, Patel DD, Murphy PM. Chemokine receptor mutant CX3CR1-M280 has impaired adhesive function and correlates with protection from cardiovascular disease in humans. *J Clin Invest.* 2003;111(8):1241-1250.
16. Xu J, Kimball TR, Lorenz JN, Brown DA, Bauskin AR, Klevitsky R, Hewett TE, Breit SN, Molkentin JD. GDF15/MIC-1 functions as a protective and antihypertrophic factor released from the myocardium in association with SMAD protein activation. *Circ Res.* 2006;98(3):342-350.
17. Kempf T, Eden M, Strelau J, Naguib M, Willenbockel C, Tongers J, Heineke J, Kotlarz D, Xu J, Molkentin JD, Niessen HW, Drexler H, Wollert KC. The transforming growth factor-beta superfamily member growth-differentiation factor-15 protects the heart from ischemia/reperfusion injury. *Circ Res.* 2006;98(3):351-360.
18. Wollert KC, Kempf T, Lagerqvist B, Lindahl B, Olofsson S, Allhoff T, Peter T, Siegbahn A, Venge P, Drexler H, Wallentin L. Growth Differentiation Factor 15 for Risk Stratification and Selection of an Invasive Treatment Strategy in Non ST-Elevation Acute Coronary Syndrome. *Circulation.* 2007.
19. Wollert KC, Kempf T, Peter T, Olofsson S, James S, Johnston N, Lindahl B, Horn-Wichmann R, Brabant G, Simoons ML, Armstrong PW, Califf RM, Drexler H, Wallentin L. Prognostic value of growth-differentiation factor-15 in patients with non-ST-elevation acute coronary syndrome. *Circulation.* 2007;115(8):962-971.
20. Soto-Cerrato V, Vinals F, Lambert JR, Perez-Tomas R. The anticancer agent prodigiosin induces p21WAF1/CIP1 expression via transforming growth factor-beta receptor pathway. *Biochem Pharmacol.* 2007;74(9):1340-1349.
21. Tzachanis D, Berezovskaya A, Nadler LM, Boussiotis VA. Blockade of B7/CD28 in mixed lymphocyte reaction cultures results in the generation of alternatively activated macrophages, which suppress T-cell responses. *Blood.* 2002;99(4):1465-1473.
22. Goerdt S, Politz O, Schledzewski K, Birk R, Gratchev A, Guillot P, Hakiy N, Klemke CD, Dippel E, Kodelja V, Orfanos CE. Alternative versus classical activation of macrophages. *Pathobiology.* 1999;67(5-6):222-226.
23. Tsou CL, Peters W, Si Y, Slaymaker S, Aslanian AM, Weisberg SP, Mack M, Charo IF. Critical roles for CCR2 and MCP-3 in monocyte mobilization from bone marrow and recruitment to inflammatory sites. *J Clin Invest.* 2007;117(4):902-909.
24. Tacke F, Alvarez D, Kaplan TJ, Jakubzick C, Spanbroek R, Llodra J, Garin A, Liu J, Mack M, van Rooijen N, Lira SA, Habenicht AJ, Randolph GJ. Monocyte subsets differentially employ CCR2, CCR5, and CX3CR1 to accumulate within atherosclerotic plaques. *J Clin Invest.* 2007;117(1):185-194.
25. Guo J, Van Eck M, Twisk J, Maeda N, Benson GM, Groot PH, Van Berkel TJ. Transplantation of monocyte

CC-chemokine receptor 2-deficient bone marrow into ApoE3-Leiden mice inhibits atherogenesis. *Arterioscler Thromb Vasc Biol.* 2003;23(3):447-453.
26. Brown DA, Moore J, Johnen H, Smeets TJ, Bauskin AR, Kuffner T, Weedon H, Milliken ST, Tak PP, Smith MD, Breit SN. Serum macrophage inhibitory cytokine 1 in rheumatoid arthritis: a potential marker of erosive joint destruction. *Arthritis Rheum.* 2007;56(3):753-764.
27. Engelse MA, Neele JM, van Achterberg TA, van Aken BE, van Schaik RH, Pannekoek H, de Vries CJ. Human activin-A is expressed in the atherosclerotic lesion and promotes the contractile phenotype of smooth muscle cells. *Circ Res.* 1999;85(10):931-939.
28. Mallat Z, Gojova A, Marchiol-Fournigault C, Esposito B, Kamate C, Merval R, Fradelizi D, Tedgui A. Inhibition of transforming growth factor-beta signaling accelerates atherosclerosis and induces an unstable plaque phenotype in mice. *Circ Res.* 2001;89(10):930-934.
29. Lutgens E, Gijbels M, Smook M, Heeringa P, Gotwals P, Koteliansky VE, Daemen MJ. Transforming growth factor-beta mediates balance between inflammation and fibrosis during plaque progression. *Arterioscler Thromb Vasc Biol.* 2002;22(6):975-982.
30. Ait-Oufella H, Salomon BL, Potteaux S, Robertson AK, Gourdy P, Zoll J, Merval R, Esposito B, Cohen JL, Fisson S, Flavell RA, Hansson GK, Klatzmann D, Tedgui A, Mallat Z. Natural regulatory T cells control the development of atherosclerosis in mice. *Nat Med.* 2006;12(2):178-180.
31. Schlittenhardt D, Schober A, Strelau J, Bonaterra GA, Schmiedt W, Unsicker K, Metz J, Kinscherf R. Involvement of growth differentiation factor-15/macrophage inhibitory cytokine-1 (GDF-15/MIC-1) in oxLDL-induced apoptosis of human macrophages in vitro and in arteriosclerotic lesions. *Cell Tissue Res.* 2004;318(2):325-333.
32. von der Thusen JH, van Vlijmen BJ, Hoeben RC, Kockx MM, Havekes LM, van Berkel TJ, Biessen EA. Induction of atherosclerotic plaque rupture in apolipoprotein E-/- mice after adenovirus-mediated transfer of p53. *Circulation.* 2002;105(17):2064-2070.
33. Guevara NV, Kim HS, Antonova EI, Chan L. The absence of p53 accelerates atherosclerosis by increasing cell proliferation in vivo. *Nat Med.* 1999;5(3):335-339.

Supplemental Figure

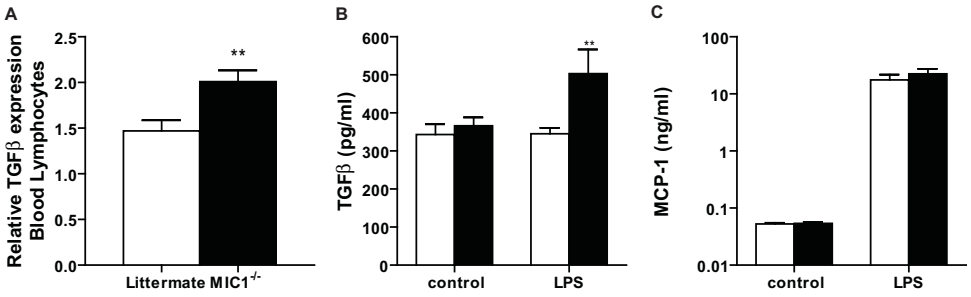

Supplemental Figure 1: *Relative TGFβ mRNA expression was increased in MIC-1$^{-/-}$ chimeras compared to littermates. Values are expressed relative to GAPDH and HPRT expression (A). Furthermore stimulation of MIC-1 deficient macrophages resulted in increased TGFβ (B), but not so much MCP-1 (C) production by these cells as assessed by ELISA. **p<0.01, ***p<0.001.*

1. Division of Biopharmaceutics, Leiden Amsterdam Center for Drug Research, Leiden University, Leiden, the Netherlands.
2. Laboratory for Psychoneuroimmunology, University Medical Center Utrecht, Utrecht, The Netherlands.
3. Experimental Vascular Pathology group, Department of Pathology, CARIM, Academic University Hospital Maastricht, the Netherlands.